ABUNDANCE OF MOSAIC PATTERNS FOR CNN WITH SPATIALLY VARIANT TEMPLATES

CHENG-HSIUNG HSU*
*Department of Mathematics, National Central University,
Chung-Li 320, Taiwan*

TING-HUI YANG
*Department of Applied Mathematics, National Chiao Tung University,
Hsinchu 30050, Taiwan*

This work investigates the complexity of one-dimensional cellular neural network mosaic patterns with spatially variant templates on finite and infinite lattices. Various boundary conditions are considered for finite lattices and the exact number of mosaic patterns is computed precisely. The entropy of mosaic patterns with periodic templates can also be calculated for infinite lattices. Furthermore, we show the abundance of mosaic patterns with respect to template periods and, which differ greatly from cases with spatially invariant templates.

Keywords: Transition matrix; spatial entropy.

1. Introduction

Cellular neural networks (CNN) are large arrays of nonlinear circuits proposed by Chua and Yang [1988a, 1988b]. Since then much work has been done in the electricial engineering community, e.g. [Chua & Roska, 1993; Thiran *et al.*, 1995]. Such systems occur as arrays of identical cells C_i that are locally connected. If the cells are sitting on lattices $Z_N := \{i \in \mathcal{Z}^1 | -N \leq i \leq N\}$, then the equation describing cell C_i at site i is as follows:

$$\frac{dx_i}{dt} = -x_i + z + a_i f(x_i)$$
$$+ \sum_{0 < |k| \leq d} a_{i;k} f(x_{i+k}), \quad i \in Z_N, \quad (1)$$

where x_{i+k}, $i + k \notin Z_N$, satisfies certain boundary conditions described below. Here, $f(x)$ is a piecewise-linear output function defined by

$$f(x) = \frac{1}{2} \left(|x + 1| - |x - 1| \right), \quad (2)$$

and $y_i = f(x_i)$ is the output of cell at i. The quantity z is called a threshold or bias term, and is related to independent voltage sources in electric circuits. The constant d is a positive integer indicating the degree of interconnection among cells. The coupling coefficients of the output functions $a_{i;k}$ and a_i are real constants called spatially variant A-templates and are denoted by

$$A_i \equiv [a_{i;-d}, \ldots, a_{i;-1}, a_i, a_{i;1}, \ldots, a_{i;d}]. \quad (3)$$

Recently, theoretical and applied studies of the CNN model have focused on lattice dynamical systems [Hsu & Lin, 2000]. A basic and important class of solutions of (1) are the stable stationary solutions. Hence, related problems can be studied by

examining two types of stationary solutions: mosaic and transitional. A mosaic solution x satisfies $|x_i| > 1$ for all $i \in \mathcal{Z}^1$ and a transitional solution satisfies $|x_i| \geq 1$ for all $i \in \mathcal{Z}^1$ and equality holds for some i. Their corresponding patterns y are called respectively mosaic and transitional patterns. Two other types of stationary solutions exist: defective and linear. A defect solution x satisfies $|x_i| > 1$ for $i \in \mathcal{Z}^1 \backslash D$ and $|x_k| < 1$ for $k \in D$, where $D \neq \emptyset$ and $D \neq \mathcal{Z}^1$. x is a linear solution if $|x_i| < 1$ for all $i \in \mathcal{Z}^1$.

The outputs $y = (f(x_i))$, called patterns, are essential for understanding CNN systems. If the templates of (1) are spatially invariant, i.e. $A_i = [r, p, s]$ for all i, then many stationary solution spatial chaos results are obtained, see e.g. [Thiran, 1997; Juang & Lin 2000; Hsu, 2000]. In this work, we are interested in studying the numbers of stationary solutions of (1) on finite lattices and infinite lattices with spatially variant templates.

Since a practical CNN has finitely many cells, some boundary conditions (B.C.) must be imposed and realized. Here, we consider three types of boundary conditions: periodic, Neumann and Dirichlet. Below, conditions are illustrated for 1-D CNN with $d = 1$.

(I)   Periodic B.C.

The cell at the right-most and the one at the left-most are connected to form a circular array. Specifically,

$$x_{-N-1}(t) = x_N(t)$$

and $$x_{N+1}(t) = x_{-N}(t)\,.$$ (P.B.C.)

(II)   Neumann B.C.

This is the zero-flux or reflective B.C., that is,

$$x_{-N-1}(t) = x_{-N}(t)$$

and $$x_{N+1}(t) = x_N(t)\,.$$ (N.B.C.)

(III)   Dirichlet B.C.

The absent cells x_{-N-1} and x_{N+1} are set to constants such that

$$x_{-N-1}(t) = \tilde{x}_{-N-1}\,,$$
$$x_{N+1}(t) = \tilde{x}_{N+1}\,.$$ (D.B.C)

Here, $\tilde{x}_{-N-1}$ and $\tilde{x}_{N+1}$ are constants with $|\tilde{x}_{-N-1}| > 1$ and $|\tilde{x}_{-N-1}| > 1$.

By using the notation for transition matrices and boundary matrices (see Sec. 3), we can obtain the exact number of mosaic patterns formed by finite cells with spatially variant templates, and which generalize the work of [Ban *et al.*, 2001b].

Let $\{M_i\}_{i=-N}^{i=N}$, L^S, and R^S be, respectively, the transition matrices of states $\{x_i\}_{i=-N}^{i=N}$, boundary matrix of x_{-N} and boundary matrix of x_N (see Sec. 3). Here $S = P$, D, or, N if the boundary conditions considered are, respectively, periodic, Dirichlet or Neumann. We also denote $[M]_{i,j}$ as the ij-entry of matrix M. The main results are as follows.

Theorem 1 (Finite cells).   *Consider mosaic patterns of (1)–(3) on Z_N with various boundary conditions. Then the number $\Gamma(Z_N)$ of mosaic patterns of (1) on Z_N is equal to*

$$\Gamma(Z_N) = \sum_{i,j=1}^{4} \left[L^S \cdot \prod_{-N+1}^{N-1} M_k \cdot R^S \right]_{i,j}\,.$$

Below, we use the symbols "+" and "−" to represent positive and negative saturated states as well as their output patterns, i.e. $y_i = +$ or $−$ if $x_i > 1$ or $x_i < 1$. Therefore, the elements in $\{+, -\}^{Z_N}$, give all possible mosaic patterns on Z_N. The results regarding the number of mosaic patterns with spatially invariant template in [Thiran, 1997] and [Ban *et al.*, 2001b] can be recovered using the above theorem.

Notably, the patterns obtained on finite lattice Z_N can be considered restrictions of global mosaic patterns on $\mathcal{Z}^1$, see [Shih, 2000]. Therefore, it is important to investigate the behavior or complexity of numbers of mosaic patterns on Z_N when N tends toward infinity. One quantity crucial to the study of behavior is spatial entropy, see Definition 4.1 [Chow & Mallet-Paret, 1995] or [Robinson, 1995]. According to Theorem 1, the entropy of mosaic patterns of (1) with spatially periodic templates (see Sec. 4) can be computed exactly as follows.

Theorem 2 (Infinite cells).   *Let ℓ and τ be positive integers and $\{A_i\}_{i=1}^{\ell\tau}$ be spatial periodic templates on finite lattice $\{i\}_{i=1}^{i=\ell\tau}$ with period τ. Denote matrix $M(\tau) = \prod_{j=1}^{j=\tau} M_j$, the entropy of mosaic patterns of (1) will then be equal to $1/\tau \ln \lambda_\tau$. Here, λ_τ is the largest positive maximal eigenvalue of $M(\tau)$.*

The rest of this paper is organized as follows. In Sec. 2, the conditions of the existence of feasible local patterns are given. According to these conditions, the parameters space of (1) can be partitioned

into finite many regions such that feasible local patterns in each region can be determined. Section 3 constructs the transition matrices and boundary matrices in the case of spatially variant templates, and shows that the number of mosaic patterns on finite cells can be computed precisely. In Sec. 4, we obtain the entropy of mosaic patterns for spatially periodic templates and give some numerical results.

2. Partition of the Parameter Space

To construct mosaic patterns on Z_N, we need to determine the number of feasible local patterns for each cell.

Definition 2.1. Denote $N_d(0) = \{k| - d \leq k \leq d\}$.

(i) A set $\Im \subset Z_N$ is called feasible if $\Im = \Im_d(i) \equiv \{i + k|k \in N_d(0)\}$ for some $i \in Z_N$.

(ii) A feasible (mosaic) solution is a vector $\{x_{i+k}\}_{k \in N_d}$ defined on a feasible set $\Im_d(i)$, with each $|x_{i+k}| > 1$, which satisfies the equations in (1).

(iii) The output patterns corresponding to feasible solutions are called feasible local patterns.

In this section, we partition the parameter space of (1) into finite many regions such that feasible local patterns can be determined in each region. Consider the general one-dimensional spatially variant templates,

$$A_i = [a_{i;-d} \cdots a_{i;-1} a_i a_{i;1} \cdots a_{i;d}].$$

For a given mosaic solution x, the state at cell C_i is $+$, i.e. $x_i > 1$, if and only

$$\sum_{0 < |k| \leq d} a_{i;k} y_{i+k} + a_i + z - 1 > 0. \qquad (4)$$

Similarly, the state at cell C_i is $-$, i.e. $x_i < -1$, if and only if

$$\sum_{0 < |k| \leq d} a_{i;k} y_{i+k} - a_i + z + 1 < 0. \qquad (5)$$

Herein, $y_{i+k}, i + k \notin Z_N$, are determined from the imposed boundary conditions. Therefore, the set of feasible local patterns for state x_i with template A_i and bias z is

$$\Omega(A_i; z) := \Omega^+(A_i, z) \cup \Omega^-(A_i, z),$$

where

$$\Omega^+(A_i, z) = \left\{ (y_{i-d} \cdots y_{i-1} y_i y_{i+1} \cdots y_{i+d})| \right.$$

$$\left. \sum_{0 < |k| \leq d} a_{i;k} y_{i+k} + a_i + z - 1 > 0 \right\},$$

$$\Omega^-(A_i, z) = \left\{ (y_{i-d} \cdots y_{i-1} y_i y_{i+1} \cdots y_{i+d})| \right.$$

$$\left. \sum_{0 < |k| \leq d} a_{i;k} y_{i+k} - a_i + z + 1 < 0 \right\}.$$

For convenience, we assume $d = 1$ and $A_i = [r_i, p_i, s_i]$ for the remainder of this work. According to (4) and (5), we can denote the eight feasible local patterns and lines for each cell as

$$(\text{i})_i \quad + \oplus +, \ z + p_i - 1 + r_i + s_i = 0,$$
$$(\text{i})_i' \quad - \ominus -, \ z - p_i + 1 - r_i - s_i = 0,$$
$$(\text{ii})_i \quad - \oplus +, \ z + p_i - 1 - r_i + s_i = 0,$$
$$(\text{ii})_i' \quad + \ominus -, \ z - p_i + 1 + r_i - s_i = 0,$$
$$(\text{iii})_i \quad + \oplus -, \ z + p_i - 1 + r_i - s_i = 0,$$
$$(\text{iii})_i' \quad - \ominus +, \ z - p_i + 1 - r_i + s_i = 0,$$
$$(\text{iv})_i \quad - \oplus -, \ z + p_i - 1 - r_i - s_i = 0,$$
$$(\text{iv})_i' \quad + \ominus +, \ z - p_i + 1 + r_i + s_i = 0.$$

Thus, in each region of the (r_i, s_i) plane as shown in Fig. 1, the $(z, p_i - 1)$ plane can be partitioned into twenty-five regions. For example, when $s_i > r_i > 0$, we have the bifurcation diagram shown in Fig. 2. From Fig. 2, if the template $A_i \in [m, n]_i$, $0 \leq m, n \leq 4$, then the feasible local patterns for (1) are as listed in Table 1.

Such a partitioning was studied in [Juang & Lin, 2000] and [Hsu *et al.*, 2000] for one-dimensional
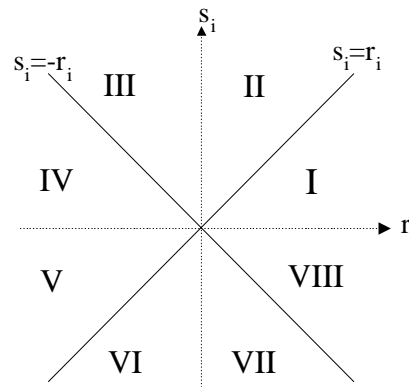

Fig. 1. Partition of the (r_i, s_i) plane.

Table 1.   Feasible local patterns for $A_i \in [m, n]_i$.

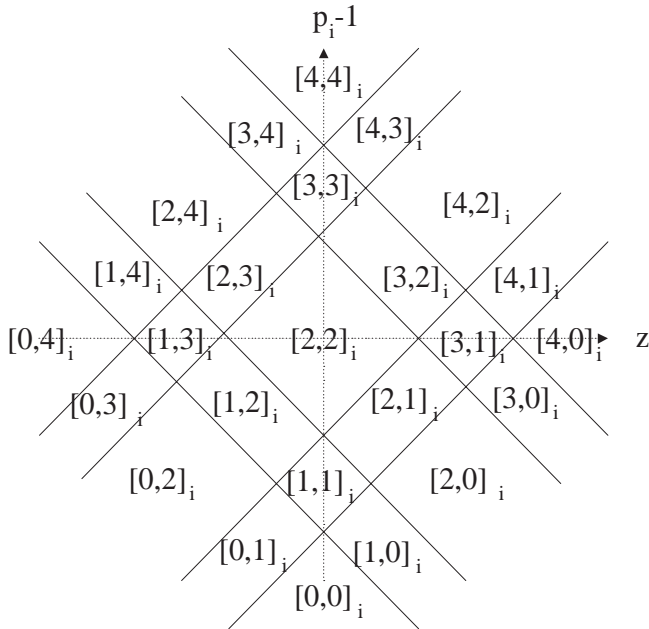| m	Feasible Local Patterns	n	Feasible Local Patterns
4	$+\oplus+, -\oplus+, +\oplus-, -\oplus-$	4	$-\ominus-, +\ominus-, -\ominus+, +\ominus+$
3	$+\oplus+, -\oplus+, +\oplus-$	3	$-\ominus-, +\ominus-, -\ominus+$
2	$+\oplus+, -\oplus+$	2	$-\ominus-, +\ominus-$
1	$+\oplus+$	1	$+\oplus+$
0	None	0	None

Fig. 2.   Partition of $(z, p_i - 1)$ plane when $0 < r_i < s_i$.

and two-dimensional CNN with spatially invariant templates. As Fig. 2 shows, there are various sets of parameters (A_i, z) by which the corresponding sets of feasible local patterns are identical. In order to obtain the feasible patterns on Z_N, we need to glue such feasible local patterns cell by cell. Hence, some transition conditions for the interior cells and boundary conditions for the boundary cells are needed to match in the following section.

3. Transition and Boundary Matrices

In this section, we construct a scheme for obtaining the feasible patterns on Z_N. This scheme can be exactly implemented by formulating suitable transitions and boundary matrices. Consequently, the number of patterns on a finite lattice with certain boundary conditions can be computed precisely.

3.1. *Transition matrix*

Firstly, we identify the indices $\{1, 2, 3, 4\}$ and the four 1×2 patterns $\{++, +-, -+, --\}$ using

$$1 \longleftrightarrow ++, \quad 2 \longleftrightarrow +-,$$
$$3 \longleftrightarrow -+, \quad 4 \longleftrightarrow --. \tag{6}$$

For simplicity, if $i \in \{1, 2, 3, 4\}$ then denote i^+ and i^-, respectively, as the left and right patterns of i in (6). For example, $2^+ = +$ and $2^- = -$. As shown in Table 1, the transition matrix $M_i \equiv M_{i;m_k,n_k}$ of state x_i with template $A_i \in [m_k, n_k]_i$, $0 \le m_k$, $n_k \le 4$ will be of the form

$$
M_{i;m_k,n_k} =
\begin{array}{c}
\\
++ \\
+- \\
-+ \\
--
\end{array}
\begin{array}{cccc}
++ & +- & -+ & -- \\
\left[\begin{array}{cccc}
m_{1,1} & m_{1,2} & 0 & 0 \\
0 & 0 & m_{2,3} & m_{2,4} \\
m_{3,1} & m_{3,2} & 0 & 0 \\
0 & 0 & m_{4,3} & m_{4,4}
\end{array}\right].
\end{array}
$$

The formation of feasible local patterns related to the transition matrix can be described as follows: the (i, j)-entry of M_i is one if and only if the jth 1×2 pattern in (6) can be joined, with one site overlapped, to the right of the ith 1×2 pattern in (6) to form a 1×3 feasible local pattern in $\Omega(A_i, z)$. Some transition matrices are listed in Table 2.

One can use these transition matrices M_i to generate patterns on lattices of lengths greater than three. For example, the nonzero $(1, 2)$-entry of $M_2 \cdot M_3$, gives the patterns $(y_1, y_2, y_3, y_4) = (+, +, +, -)$ on a 1×4 lattice. Indeed, the (i, j)-th entry of $\prod_{k=-N+1}^{N-1} M_k$ gives the number of patterns on Z_N with the ith 1×2 pattern in (6) at the two sites to the left-most of Z_N and the jth 1×2 pattern in (6) at the two sites to the right-most of Z_N. For example, when $i = 2$, $j = 4$, the patterns on Z_N are

Table 2. Transition matrices for x_i when $A_i \in [m_k, n_k]_i$, $m_k, n_k \geq 3$.

M_i	$m_{1,1}$	$m_{1,2}$	$m_{2,3}$	$m_{2,4}$	$m_{3,1}$	$m_{3,2}$	$m_{4,3}$	$m_{4,4}$
$m_k = 4, n_k = 4$	1	1	1	1	1	1	1	1
$m_k = 4, n_k = 3$	1	1	0	1	1	1	1	1
$m_k = 3, n_k = 4$	1	1	1	1	1	0	1	1
$m_k = 3, n_k = 3$	1	1	0	1	1	0	1	1

of the form,

$$\boxed{\;+\;|\;-\;|\;\cdots\cdots\;|\;-\;|\;-\;}.$$

If the states x_{-N} and x_N satisfy the imposed B.C. defined in Sec. 1, then the above construction of transition matrices allow us to count the number of mosaic patterns on Z_N. Therefore, it is necessary to describe the feasible patterns on the boundary sites with respect to the imposed B.C. using matrices called boundary matrices as shown below.

3.2. *Boundary matrices*

Assume $A_{-N} \in [m_k, n_k]_{-N}$. We use the symbols L^p(or $L^P_{m_k,n_k}$), L^N(or $L^N_{m_k,n_k}$), and L^D(or $L^D_{m_k,n_k}$) to denote the left-most boundary matrices for state x_{-N} with periodic, Neumann and Dirichlet boundary conditions, respectively. Similarly, the symbols R^p(or $R^P_{m_k,n_k}$), R^N(or $R^N_{m_k,n_k}$) and R^D(or $R^D_{m_k,n_k}$) denote the right-most boundary matrices for state

x_N with periodic, Neumann and Dirichlet boundary conditions, respectively. The boundary matrices are defined below.

3.2.1. *Periodic boundary matrices*

As defined in (6), let $\{y_k\}_{k=-N}^{k=N}$ be a pattern on Z_N such that $\{y_k\}_{k=-N+1}^{k=N-1}$ is a feasible pattern on Z_{N-1} with $\overline{y_{-N}y_{-N+1}} = i$ and $\overline{y_{N-1}y_N} = j$, $1 \leq i, j \leq 4$. If $\{x_k\}_{k=-N}^{k=N}$ satisfies the (P.B.C.), we need to check the feasibility of local patterns for cells at $-N$ and N sites. According to Fig. 3, the right-most jth 1×2 pattern can be joined to the left-most of the ith 1×2 pattern if and only if $\overline{y_N y_{-N} y_{-N+1}}$ is a feasible local pattern for cell $-N$, and the left-most ith 1×2 pattern can be joined to the right-most of the jth 1×2 pattern if and only if $\overline{y_{N-1} y_N y_{-N}}$ is a feasible local pattern for cell N. Hence, the left boundary matrix L^P and right boundary matrices R^P can be constructed as follows:

$$
L^P = \begin{array}{c} \\ ++ \\ +- \\ -+ \\ -- \end{array}
\begin{array}{c} \begin{array}{cccc} ++ & +- & -+ & -- \end{array} \\
\begin{bmatrix} \ell_{1,1} & \ell_{1,2} & 0 & 0 \\ 0 & 0 & \ell_{2,3} & \ell_{2,4} \\ \ell_{3,1} & \ell_{3,2} & 0 & 0 \\ 0 & 0 & \ell_{4,3} & \ell_{4,4} \end{bmatrix} \end{array},
\qquad
R^P = \begin{array}{c} \\ ++ \\ +- \\ -+ \\ -- \end{array}
\begin{array}{c} \begin{array}{cccc} ++ & +- & -+ & -- \end{array} \\
\begin{bmatrix} r_{1,1} & r_{1,2} & 0 & 0 \\ 0 & 0 & r_{2,3} & r_{2,4} \\ r_{3,1} & r_{3,2} & 0 & 0 \\ 0 & 0 & r_{4,3} & r_{4,4} \end{bmatrix} \end{array}.
$$

Here,

$$\ell_{k,i} = 1 \quad \text{for} \quad 1 \leq i, k \leq 4 \quad \text{if and only if}$$

$$[M_{-N}]_{k,i} \neq 0 \quad \text{and} \quad [M_N]_{j,k} \neq 0 \quad \text{for some} 1 \leq j \leq 4$$

$$\text{and} \hspace{5cm} \text{(P.B.C.)}_1$$

$$r_{j,k} = 1 \quad \text{for} \quad 1 \leq j, k \leq 4 \quad \text{if and only if}$$

$$[M_{-N}]_{k,i} \neq 0 \quad \text{and} \quad [M_N]_{j,k} \neq 0 \text{ for some} 1 \leq i \leq 4.$$

3.2.2. *Neumann boundary matrices*

Let $\{y_k\}_{k=-N}^{k=N}$ be a pattern on Z_N such that $\{y_k\}_{k=-N+1}^{k=N-1}$ is a feasible pattern on Z_{N-1} with $\overline{y_{-N}y_{-N+1}} = i$ and $\overline{y_{N-1}y_N} = j$. The Neumann boundary matrices can be similarly defined.
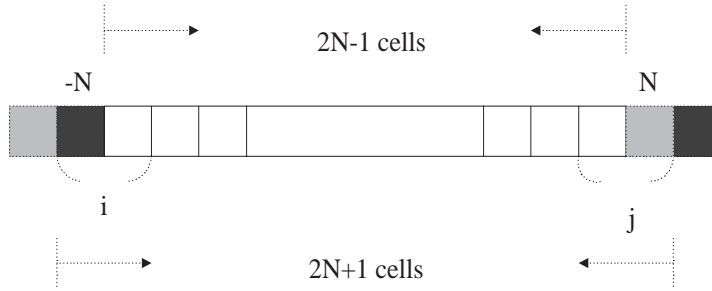
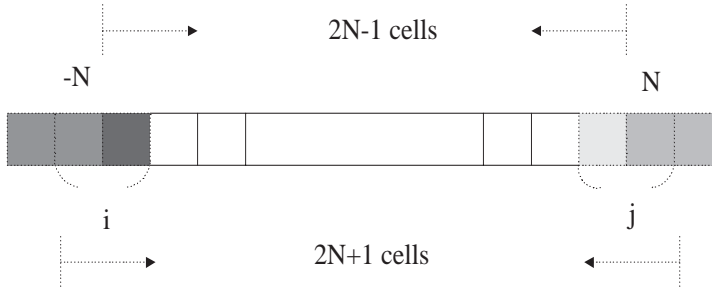Fig. 3.   Patterns with periodic boundary conditions.

Fig. 4.   Patterns for Neumann boundary conditions.

According to Fig. 4, the left boundary matrix L^N and right boundary matrices R^N are defined as follows:

$$
L^N =
\begin{array}{c}
\\ ++ \\ +- \\ -+ \\ --
\end{array}
\begin{array}{cccc}
++ & +- & -+ & -- \\
\end{array}
\left[
\begin{array}{cccc}
\ell_{1,1} & \ell_{1,2} & 0 & 0 \\
0 & 0 & 0 & 0 \\
0 & 0 & 0 & 0 \\
0 & 0 & \ell_{4,3} & \ell_{4,4}
\end{array}
\right], \qquad
R^N =
\begin{array}{c}
\\ ++ \\ +- \\ -+ \\ --
\end{array}
\begin{array}{cccc}
++ & +- & -+ & -- \\
\end{array}
\left[
\begin{array}{cccc}
r_{1,1} & 0 & 0 & 0 \\
0 & 0 & 0 & r_{2,4} \\
r_{3,1} & 0 & 0 & 0 \\
0 & 0 & 0 & r_{4,4}
\end{array}
\right].
$$

Here,

$$
\begin{aligned}
&\ell_{1,i} = 1, \ i = 1, 2 \quad \text{if and only if} \quad [M_{-N}]_{1,i} = 1\,, \\
&\ell_{4,i} = 1, \ i = 3, 4 \quad \text{if and only if} \quad [M_{-N}]_{4,i} = 1\,, \\
&r_{i,1} = 1, \ i = 1, 3 \quad \text{if and only if} \quad [M_N]_{i,1} = 1\,, \\
&r_{i,4} = 1, \ i = 2, 4 \quad \text{if and only if} \quad [M_N]_{i,4} = 1\,.
\end{aligned}
\qquad \text{(N.B.C.)}_1
$$

Some Neumann boundary matrices are listed in Table 3.

3.2.3.   *Dirichlet boundary matrices*

Let $\{y_k\}_{k=-N-1}^{k=N+1}$ be a pattern on Z_{N+1} such that $\{y_k\}_{k=-N}^{k=N}$ is a feasible pattern on Z_N with $\overline{y_{-N-1}y_{-N}} = i$ and $\overline{y_N y_{N+1}} = j$. According to Fig. 5, it is obvious that $\{y_k\}_{k=-N}^{k=N}$ satisfies (D.B.C.) if and only if i^- and j^+ are equal to the output patterns of $\tilde{y}_{-N-1}$ and $\tilde{y}_{N+1}$, respectively.

Table 3.   Neumann boundary matrices.

	$L_{m,n}^N, m, n \geq 3$	$L_{2,3}^N$	$L_{3,2}^N$	$L_{m,n}^N, 2 \geq m, n \geq 1$	$L_{1,0}^N$	$L_{0,1}^N$	$L_{0,0}^N$
$\ell_{1,1}$	1	1	1	1	1	0	0
$\ell_{1,2}$	1	0	1	0	0	0	0
$\ell_{4,3}$	1	1	0	0	0	0	0
$\ell_{4,4}$	1	1	1	1	0	1	0

Table 3. (*Continued*).

$R_{m,n}^N m, n \geq 2$	$R_{1,2}^N$	$R_{2,1}^N$	$R_{1,1}^N$	$R_{1,0}^N$	$R_{0,1}^N$	$R_{0,0}^N$
$r_{1,1}$	1	1	1	1	1	0	0
$r_{2,4}$	1	1	0	0	0	0	0
$r_{3,1}$	1	0	1	0	0	0	0
$r_{4,4}$	1	1	1	1	0	1	0

The left boundary matrix L^D and right boundary matrices R^D are defined as follows:

$$
L^D = \begin{matrix} & \begin{matrix} ++ & +- & -+ & -- \end{matrix} \\ \begin{matrix} ++ \\ +- \\ -+ \\ -- \end{matrix} & \begin{bmatrix} \ell_{1,1} & \ell_{1,2} & 0 & 0 \\ 0 & 0 & \ell_{2,3} & \ell_{2,4} \\ \ell_{3,1} & \ell_{3,2} & 0 & 0 \\ 0 & 0 & \ell_{4,3} & \ell_{4,4} \end{bmatrix} \end{matrix}, \qquad R^D = \begin{matrix} & \begin{matrix} ++ & +- & -+ & -- \end{matrix} \\ \begin{matrix} ++ \\ +- \\ -+ \\ -- \end{matrix} & \begin{bmatrix} r_{1,1} & r_{1,2} & 0 & 0 \\ 0 & 0 & r_{2,3} & r_{2,4} \\ r_{3,1} & r_{3,2} & 0 & 0 \\ 0 & 0 & r_{4,3} & r_{4,4} \end{bmatrix} \end{matrix}.
$$

Here

$$
\ell_{i,j} = 1 \quad \text{if and only if} \quad i^- = \tilde{y}_{-N-1} \text{ and } [M_{-N}]_{i,j} \neq 0 ,
$$

$$
r_{i,j} = 1 \quad \text{if and only if} \quad j^+ = \tilde{y}_{N+1} \text{ and } [M_N]_{i,j} \neq 0 .
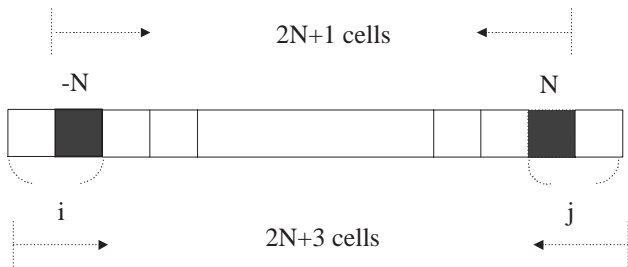$$

$$\text{(D.B.C)}_1$$

Fig. 5. Patterns with Dirichlet boundary conditions.

Using the preceding arguments, we prove Theorem 1 as follows.

Proof of Theorem 1. Proof is given only for the case of periodic boundary conditions; the other cases can be proved in similar fashion.

According to Fig. 3, let $\{y_k\}_{k=-N}^{k=N}$ be a pattern on Z_N such that $\{y_k\}_{k=-N+1}^{k=N-1}$ is a feasible pattern on Z_{N-1} with $\overline{y_{-N}y_{-N+1}} = i$ and $\overline{y_{N-1}y_N} = j$. Then the number of such feasible patterns on Z_{N-1} is equal to $[\prod_{-N+1}^{N-1} M_k]_{i,j}$. Hence, $\{y_k\}_{k=-N}^{k=N}$ is a feasible pattern on Z_N is equivalent to that $\overline{y_N y_{-N} y_{-N+1}}$ is a feasible local pattern for cell $-N$, and $\overline{y_{N-1} y_N y_{-N}}$ is a feasible local pattern for cell N. Therefore, according to the construction (P.B.C.)_1 of periodic boundary matrices, the results obviously follow. The proof is complete. ∎

If the templates considered are spatially invariant, i.e. $A_i = [r, p, s]$ for all cells, then the results of Theorem 1 replicate the results obtained by [Ban *et al.*, 2001b; Thiran, 1997]. For details see Table 4.

4. Results of Entropy

Obtaining the numbers of feasible patterns for various boundary conditions was shown in the preceding section. It is also important and interesting to study the behavior of such number with respect to the length of Z_N. One way to investigate this behavior is to compute the entropy (see [Chow & Mallet-Paret, 1995]) of stationary solutions of (1). In one-dimensional cases, the entropy function h on $\mathcal{Z}^1$ can be defined as

Definition 4.1. Let $\Gamma(Z_N)$ be the number of feasible patterns on Z_N that satisfy the imposed boundary conditions. Thus,

$$
h_N(Z_N) \equiv \frac{\ln \Gamma(Z_N)}{2N + 1}
$$

and

$$
h(\mathcal{Z}^1) \equiv \lim_{N \to \infty} \frac{\ln \Gamma(Z_N)}{2N + 1} .
$$

$h(\mathcal{Z}^1)$ is called the entropy of stationary solutions of (1). Furthermore, if $h(\mathcal{Z}^1) > 0$ or $h(\mathcal{Z}^1) = 0$ then

Table 4.   Exact number of mosaic patterns for a spatially invariant template.

Region in $r - s$ Plane	Region in $z - p$ Plane	P.B.C.	N.B.C.
	$[4, 4]$	2^H	2^H
(I), (II)	$[3, 3]$	$\Gamma_2(H)$	$\Gamma_1(H)$
	$[2, 2]$	2	2
	$[4, 4]$	2^H	2^H
(III), (VIII)	$[3, 3]$	2	2
	$[2, 2]$	0	2
	$[4, 4]$	2^H	2^H
(IV), (VII)	$[3, 3]$	2	$3 + (-1)^H$
	$[2, 2]$	0	$1 + (-1)^H$
	$[4, 4]$	2^H	2^H
(V), (VI)	$[3, 3]$	$\Gamma_2(H)$	$\Gamma_1(H)$
	$[2, 2]$	2	$1 + (-1)^H$

$$H = 2N + 1.$$

$$\Gamma_1(H) = \left[\left(\frac{1 + \sqrt{5}}{2} \right)^H + \left(\frac{1 - \sqrt{5}}{2} \right)^H \right] + 2 \cos \left(\frac{2\pi}{3} H \right).$$

$$\Gamma_2(H) = \frac{2}{\sqrt{5}} \left[\left(\frac{1 + \sqrt{5}}{2} \right)^{H+1} - \left(\frac{1 - \sqrt{5}}{2} \right)^{H+1} \right].$$

(1) is said to be spatial chaos or pattern formation, respectively.

Shih [2000] proved that boundary conditions have negligible influence on pattern formation and spatial chaos of mosaic patterns of (1) with spatially invariant templates. If fact, by the same arguments, the results also hold for the case of spatially variant templates.

If the templates are spatially invariant, according to [Juang & Lin, 2000], the entropy h of mosaic patterns on $\mathcal{Z}^1$ is

$$h = \begin{cases} \ln 2 & \text{if } (z, p) \in [4, 4], \\ \ln \lambda & \text{if } (z, p) \in [4, 3] \text{ or } [3, 4], \\ \ln \dfrac{1 + \sqrt{5}}{2} & \text{if } (z, p) \in [3, 3], \\ 0 & \text{otherwise}. \end{cases} \quad (7)$$

Here, λ is the maximal root of $\lambda^3 - 2\lambda^2 + \lambda - 1 = 0$.

On the other hand, if the templates are spatially variant, the structure of the entropy function is quite different. Some partial entropy will appear for different combinations of templates. For instance, if we assume one template for odd cells

and another template for even cells, then the entropy h on $\mathcal{Z}^1$ is computed as follows.

Example 4.1.   Let $N \geq 3$ be a positive integer and

$$A_k = [r_k, p_k, s_k] \in \begin{cases} [4, 1], & \text{if } k \text{ is odd}, \\ [1, 4], & \text{if } k \text{ is even}, \end{cases} \quad (8)$$

on Z_N. If we consider the mosaic patterns of (1) on Z_N with different boundary conditions imposed as in previous section, then the entropy functions are equal. Moreover, we have

$$h(\mathcal{Z}^1) = \ln \frac{1 + \sqrt{5}}{2}.$$

Proof.   Without lost of generality, we may assume $Z_N = \{i\}_{i=1}^{i=N}$. First, let $\{S(K)\}_{K=1}^{\infty}$ be a Fibonacci sequence, i.e.

$$S(1) = 1, \quad S(2) = 2,$$

and

$$S(K + 2) = S(K + 1) + S(K), \quad \text{if } K \geq 1.$$

It is well known that

$$S(K) = \frac{1}{\sqrt{5}} \left[\left(\frac{1+\sqrt{5}}{2} \right)^K - \left(\frac{1-\sqrt{5}}{2} \right)^K \right]. \quad (9)$$

Using (8), if $K \geq 3$ then it is not difficult to compute that

$$\prod_{k=2}^{2K} M_k = \begin{bmatrix} S(2K-4) & 0 & S(2K-3) & S(2K-3) \\ S(2K-3) & 0 & S(2K-2) & S(2K-2) \\ 0 & 0 & 0 & 0 \\ S(2K-3) & 0 & S(2K-2) & S(2K-2) \end{bmatrix},$$

$$(10)$$

$$\prod_{k=2}^{2K-1} M_k = \begin{bmatrix} S(2K-4) & S(2K-4) & 0 & S(2K-5) \\ S(2K-3) & S(2K-3) & 0 & S(2K-4) \\ 0 & 0 & 0 & 0 \\ S(2K-3) & S(2K-3) & 0 & S(2K-4) \end{bmatrix},$$

and

$$\sum_{i,j=1}^{4} \left[\prod_{k=2}^{K-1} M_k \right]_{i,j} = S(K+1). \quad (11)$$

The numbers $\Gamma(Z_N)$ for different boundary conditions are computed below.

Case (**I**) (**P.B.C.**). Since the L^P, R^P on Z_N in Theorem 1 can be presented as

$$L^P = \begin{bmatrix} 1 & 1 & 0 & 0 \\ 0 & 0 & 0 & 0 \\ 0 & 0 & 0 & 0 \\ 0 & 0 & 0 & 1 \end{bmatrix},$$

and

$$R^P = \begin{bmatrix} 1 & 0 & 0 & 0 \\ 0 & 0 & 0 & 0 \\ 1 & 0 & 0 & 0 \\ 0 & 0 & 0 & 1 \end{bmatrix}, \text{ if } N \text{ is odd, and}$$

$$L^P = \begin{bmatrix} 1 & 1 & 0 & 0 \\ 0 & 0 & 0 & 0 \\ 1 & 1 & 0 & 0 \\ 0 & 0 & 1 & 1 \end{bmatrix},$$

and

$$R^P = \begin{bmatrix} 1 & 0 & 0 & 0 \\ 0 & 0 & 1 & 1 \\ 0 & 0 & 0 & 0 \\ 0 & 0 & 1 & 1 \end{bmatrix}, \text{ if } N \text{ is even,}$$

by (10), we have

$$\Gamma(Z_{2K+1}) = S(2K+2), \quad K \geq 3,$$

and

$$\Gamma(Z_{2K}) = S(2K+3), \quad K \geq 3.$$

Case (**II**) (**N.B.C.**). Elementary computation yields

$$L^N = \begin{bmatrix} 1 & 1 & 0 & 0 \\ 0 & 0 & 0 & 0 \\ 0 & 0 & 0 & 0 \\ 0 & 0 & 0 & 1 \end{bmatrix}, \quad R^N = \begin{bmatrix} 1 & 0 & 0 & 0 \\ 0 & 0 & 0 & 1 \\ 0 & 0 & 0 & 0 \\ 0 & 0 & 0 & 1 \end{bmatrix},$$

and

$$R^N = \begin{bmatrix} 1 & 0 & 0 & 0 \\ 0 & 0 & 0 & 0 \\ 1 & 0 & 0 & 0 \\ 0 & 0 & 0 & 1 \end{bmatrix}.$$

Hence, using Theorem 1 and (9), we obtain

$$\Gamma(Z_{2K+1}) = S(2K+2), \quad K \geq 3,$$

and

$$\Gamma(Z_{2K}) = S(2K+1), \quad K \geq 3.$$

Case (**III**) (**D.B.C.**). In this case, we consider $f(\tilde{x}_0) = 1$ and $f(\tilde{x}_{N+1}) = 1$. The other cases can also be investigated in similar fashion. Using Theorem 1, it is easy to determine that

$$L^D = \begin{bmatrix} 1 & 1 & 0 & 0 \\ 0 & 0 & 0 & 0 \\ 0 & 0 & 0 & 0 \\ 0 & 0 & 0 & 0 \end{bmatrix}, \quad R^D = \begin{bmatrix} 1 & 0 & 0 & 0 \\ 0 & 0 & 1 & 0 \\ 0 & 0 & 0 & 0 \\ 0 & 0 & 1 & 0 \end{bmatrix},$$

and

$$R^D = \begin{bmatrix} 1 & 0 & 0 & 0 \\ 0 & 0 & 0 & 0 \\ 1 & 0 & 0 & 0 \\ 0 & 0 & 0 & 0 \end{bmatrix}.$$

Therefore,

$$\Gamma(Z_{2K+1}) = \Gamma(Z_{2K}) = S(2K), \quad K \geq 3.$$

Consequently, according to Definition 4.1 and (9) and the computations above, we have $h(\mathcal{Z}^1) = \ln(1+\sqrt{5})/2$. The proof is complete. ∎

Remark 4.1.

(i) The preceding example shows the influence of boundary conditions on pattern formation and spatial chaos is negligible. In general, this is also true for any type of spatially variant templates. For details, see [Shih, 2000].

(ii) According to (7), entropy is equal to zero if the template is spatially invariant in region $[4, 1]$ or $[1, 4]$. However, the entropy obtained in Example 4.1 is equal to the entropy obtained by [Juang & Lin, 2000] in region $[3, 3]$ although the patterns are quite different. Therefore, the structure of entropy is more complicated when templates are spatially variant.

Motivated by Example 4.1, we introduce a definition of periodic templates and prove Theorem 2 below. For simplicity, we consider the finite lattices $Z_N = \{k\}_{k=1}^{k=N}$ and $\Gamma(Z_N) = \sum_{i,j=1}^{4} [\prod_{k=1}^{N} M_k]_{i,j}$ hereinafter.

Definition 4.2.   Let ℓ and τ be positive integers. The family of templates $A_i = [r_i, p_i, s_i] \in [m_i, n_i]_i$, $i = 1$ to $\ell\tau$ are called spatially periodic on $Z_{\ell\tau}$ with period τ if

$$m_i = m_j \text{ and } n_i = n_j, \quad \text{for } i = j \pmod{\tau}.$$

Here, $1 \le j \le \tau$, $1 \le i \le \ell\tau$ and $0 \le m_i, n_i \le 4$.

Proof of Theorem 2.   When $\tau = 1$, according to [Chow & Mallet-Paret, 1995], we have

$$\lim_{\ell\to\infty} h_\ell(Z_\ell) = \lim_{\ell\to\infty} \frac{1}{\ell} \sum_{i,j=1}^{4} \left[\prod_{k=1}^{\ell} M(1) \right]_{i,j} = \ln \lambda_1,$$

where λ_1 is the largest positive maximal eigenvalue of $M(1)$. From Theorem 1, we obtain

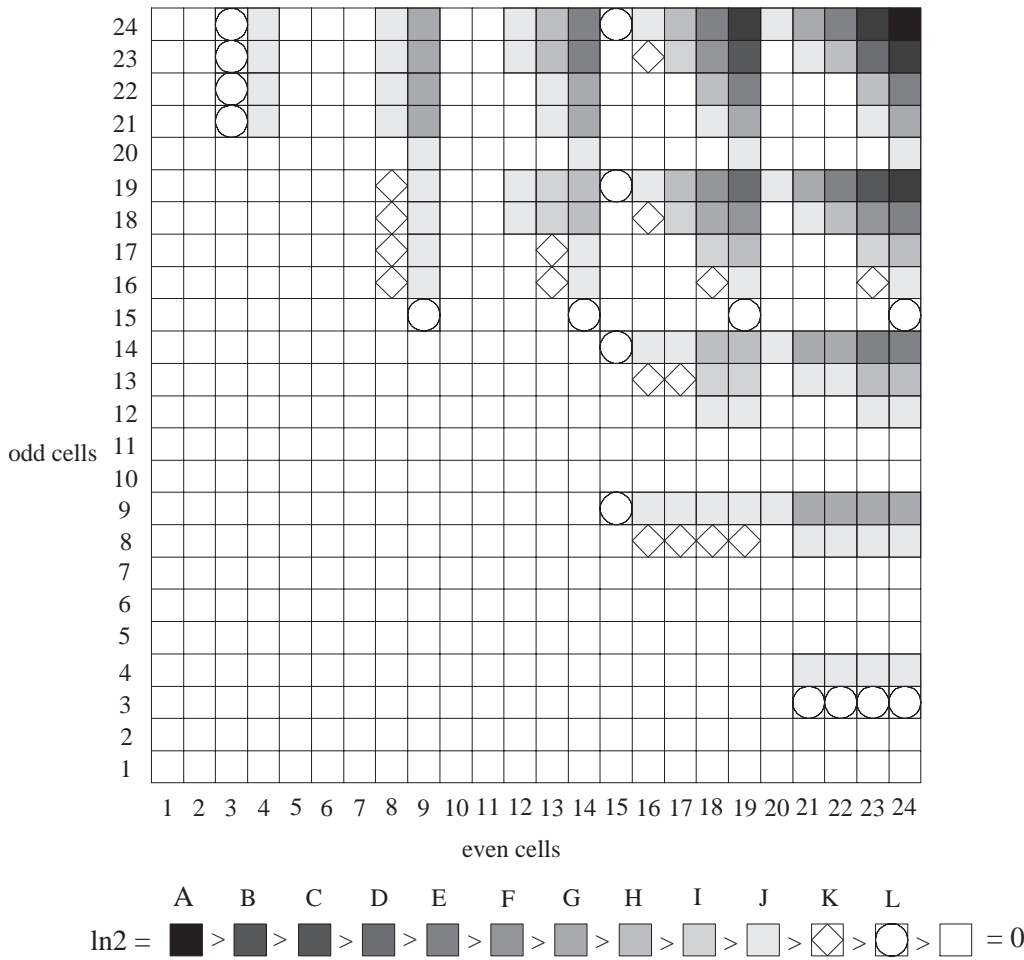$$\Gamma(Z_{\ell\tau}) = \sum_{i,j=1}^{4} \left[\prod_{k=1}^{\ell} M(\tau) \right]_{i,j}$$

Fig. 6.   Structure of $h(\mathcal{Z}^1)$ when $\tau = 2$.

Table 5.   Characteristic equations, exact entropy and numerical results.

Class	P(2)	$h(\mathcal{Z}^\infty) = \frac{1}{2}\ln\lambda_2$	$h_{1000}(Z_{1000})$
A	$\lambda^4 - 4\lambda^3$	0.6931	0.6945
B	$\lambda^4 - 3\lambda^3 - 2\lambda^2$	0.6350	0.6366
C	$\lambda^4 - 3\lambda^3 - \lambda^2 - \lambda$	0.6094	0.6109
D	$\lambda^4 - 2\lambda^3 - 3\lambda^2 - \lambda$	0.5624	0.5640
E	or (i) $\lambda^4 - 2\lambda^3 - 3\lambda^2$ (ii) $\lambda^4 - 3\lambda^3$	0.5493	0.5510
F	$\lambda^4 - 2\lambda^3 - 2\lambda^2 - \lambda$	0.5203	0.5220
G	or (i) $\lambda^4 - 2\lambda^3 - \lambda^2 - 2\lambda + 1$ (ii) $\lambda^4 - 3\lambda^3 + \lambda^2$	0.4812	0.4830
H	$\lambda^4 - 2\lambda^3 - \lambda^2$	0.4407	0.4426
I	$\lambda^4 - 2\lambda^3 - \lambda$	0.3955	0.3975
J	$\lambda^4 - 2\lambda^3$	0.3466	0.3486
K	$\lambda^4 - 2\lambda^3 + \lambda^2 - \lambda$	0.2812	0.2834
L	$\lambda^4 - \lambda^3 - \lambda^2$	0.2406	0.2428

Table 6.   Numerical results for $h(\mathcal{Z}^1)$ with $3 \leq \tau \leq 6$.

τ	$T(\tau)$	$P(\tau)$	$DP(\tau)$	$C(\tau)$
1	25^1	4	3	3
2	25^2	152	14	12
3	25^3	4420	33	27
4	25^4	121456	90	84
5	25^5	3209404	214	195
6	25^6	82014632	577	497

and

$$\lim_{\ell \to \infty} h_\ell(Z_{\ell\tau}) = \lim_{\ell \to \infty} \frac{\Gamma(Z_{\ell\tau})}{\ell\tau} = \frac{1}{\tau}\ln\lambda_\tau \,.$$

The proof is complete.   ∎

Since the function $\eta(m,n) = 5m + n$ is an one-to-one function from $\{0,1,2,3,4\} \times \{0,1,2,3,4\}$ onto $\{0,1\ldots,24\}$, we may denote $[m,n]$ as $\eta(m,n)$. When $\tau = 2$, there are 152 combinations of templates with positive entropy. Among these there are 14 distinct characteristic polynomials with positive entropy and 12 distinct positive entropies.

The structure of $h(\mathcal{Z}^1)$ is illustrated in Fig. 6 by replacing x-, y-axis with $\eta(m,n)$ respectively.

The characteristic equations, $h(\mathcal{Z}^1)$ and h_N for $N = 1000$ are also listed in Table 5.

Remark 4.2. Some numerical results are listed in Table 6 for the case of $3 \leq \tau \leq 6$ with:

$T(\tau) \equiv$ total combination of templates,

$P(\tau) \equiv$ all combinations of templates with positive entropy,

$DP(\tau) \equiv$ distinct characteristic polynomials with positive entropy,

$C(\tau) \equiv$ distinct positive entropies.

Acknowledgment

References

Ban, R. C., Jane, K. P., Hsu, C.-H. & Lin, S.-S. [2001a], "Spatial disorder of cellular neural networks with asymmetric output function," *Int. J. Bifurcation and Chaos* **11**(8) 2085–2095.

Ban, R. C., Lin, S.-S. & Shih, C.-W. [2001b] "Exact number of mosaic patterns in cellular neural networks," *Int. J. Bifurcation and Chaos* **11**(6), 1645–1653.

Chow, S.-N. & Mallet-Paret, J. [1995] "Pattern formation and spatial chaos in lattice dynamical system," *IEEE Trans. Circuits Syst.* **42**, 746–751.

Chow, S.-N., Mallet-Paret, J. & Van Vleck, E. S. [1996] "Pattern formation and spatial chaos in spatially discrete evolution equations," *Rand. Comput. Dyn.* **4**, 109–178.

Chua, L. O. & Yang, L. [1988a] "Cellular neural networks: Theory," *IEEE Trans. Circuits Syst.* **35**, 1257–1272.

Chua, L. O. & Yang, L. [1988b] "Cellular neural networks: Applications," *IEEE Trans. Circuits Syst.* **35**, 1273–1290.

Chua, L. O. & Roska, T. [1993] "The CNN paradigm," *IEEE Trans. Circuits Syst.* **40**, 147–156.

Chua, L. O. [1998] *CNN: A Paradigm for Complexity*, World Scientific Series on Nonlinear Science, Series A, Vol. 31.

Hsu, C.-H. [2000] "Smale horseshoe of cellular neural networks," *Int. J. Bifurcation and Chaos* **10**(12), 2119–2129.

Hsu, C.-H. & Lin, S.-S. [2000] "Existence and multiplicity of traveling waves in lattice dynamical system," *J. Diff. Eqns.* **164**, 431–450.

Hsu, C.-H., Juang, J., Lin, S.-S. & Lin, W.-W. [2000] "Cellular neural networks: Local patterns for general templates," *Int. J. Bifurcation and Chaos* **10**(7), 1645–1659.

Juang, J. & Lin, S.-S. [2000] "Cellular neural networks: Mosaic pattern and spatial chaos," *SIAM J. Appl. Math.* **60**, 891–915.

Robinson, C. [1995] *Dynamical Systems* (CRC Press, Boca Raton, FL).

Shih, C.-W. [2000] "Influence of boundary conditions on pattern formation and spatial chaos for lattice dynamical systems," *SIAM J. Appl. Math.* **61**(1), 335–368.

Thiran, P., Crounse, K. B., Chua, L.O. & Hasler, M. [1995] "Pattern formation properties of autonomous cellular neural networks," *IEEE Trans. Circuits Syst.* **42**, 757–774.

Thiran, P. [1997] *Dynamics and Self-Organization of Locally Coupled Neural Networks* (Press Polytechniques et Universitaires Romandes, Lausanne, Switzerland).

This article has been cited by:

1. Jung-Chao Ban. 2014. Neural network equations and symbolic dynamics. *International Journal of Machine Learning and Cybernetics* . [CrossRef]

2. YUN-QUAN KE, CHUN-FANG MIAO. 2010. EXISTENCE ANALYSIS OF STATIONARY SOLUTIONS FOR RTD-BASED CELLULAR NEURAL NETWORKS. *International Journal of Bifurcation and Chaos* **20**:07, 2123-2136. [Abstract] [References] [PDF] [PDF Plus]

3. JUNG-CHAO BAN, CHIH-HUNG CHANG. 2008. ON THE DENSE ENTROPY OF TWO-DIMENSIONAL INHOMOGENEOUS CELLULAR NEURAL NETWORKS. *International Journal of Bifurcation and Chaos* **18**:11, 3221-3231. [Abstract] [References] [PDF] [PDF Plus]

4. YUNQUAN KE. 2008. THE MOSAIC PATTERNS OF CNN WITH SYMMETRIC FEEDBACK TEMPLATE. *International Journal of Bifurcation and Chaos* **18**:02, 375-390. [Abstract] [References] [PDF] [PDF Plus]

5. YUN-QUAN KE, FENG-YAN ZHOU. 2006. EXISTENCE ANALYSIS OF MOSAIC SOLUTIONS FOR ONE-DIMENSIONAL CELLULAR NEURAL NETWORKS. *International Journal of Bifurcation and Chaos* **16**:12, 3669-3677. [Abstract] [References] [PDF] [PDF Plus]

6. SONG-SUN LIN, WEN-WEI LIN, TING-HUI YANG. 2004. BIFURCATIONS AND CHAOS IN TWO-CELL CELLULAR NEURAL NETWORKS WITH PERIODIC INPUTS. *International Journal of Bifurcation and Chaos* **14**:09, 3179-3204. [Abstract] [References] [PDF] [PDF Plus]